VNU Journal of Science: Natural Sciences and Technology, Vol. 42, No. 4 (2026) 53-61

VNU Journal of Science: Natural Sciences and Technology

Journal homepage: https://js.vnu.edu.vn/NST

Original Article

Study on the Spectroscopy Properties of Nitrogen Doped Graphene Quantum Dots And Sulfur - Nitrogen Co-Doped Graphene Quantum Dots

Le Xuan Hung[1,2,*], Pham Thu Nga[2,3], Nguyen Thi Mai Huong[4]

[1]*Institute of Research and Development, Duy Tan University, Da Nang, Vietnam*
[2]*School of Engneering and Technology, Duy Tan University, Da Nang, Vietnam*
[3]*Institute of Theoretical and Applied Research, Duy Tan University, Hanoi, Vietnam*
[4] *Institute of Physics, Vietnam Academy of Science and Technology, Hanoi, Vietnam*

Received 01st May 2025
Revised 23rd August 2026; Accepted 28th August 2026

Abstract: In this work, we present a method to fabricate nitrogen-doped Graphene (N-GQDs) and sulfur - nitrogen co-doped graphene quantum dots (S,N-GQDs) and investigate their optical properties. The GQDs are prepared using a microwave-assisted hydrothermal method, which is a simple, environmentally friendly approach that allows for easy dispersion in water and quick application. Structural and morphological analyses reveal that the material has a nanostructure with a size ranging from approximately 4.5 to 9.5 nm and their characteristic bonds are present. The effects of different dopants in GQDs crystal lattice on the optical properties are also systematically analyzed. Additionally, we provide an in-depth discussion of the luminescence mechanism.

Keywords: Graphene quantum dots, N-GQDs, S,N-GQDs, hydrothermal, photoluminescence spectra, EEM.

1. Introduction

Graphene, a two-dimensional (2D) honeycomb lattice of sp^2-bonded carbon atoms, has a zero band gap, which has limited its applications in many fields. New properties and applicability only emerge when graphene transforms from its native 2D structure into a 0D (graphene quantum dot) [1] or 1D (graphene nanoribbon) form [2]. With graphene quantum dots (GQDs) smaller than 10 nm in size, quantum confinement and edge effects become significant, leading to the expansion of the band gap. As a result, GQDs exhibit special properties such as fluorescence, high biocompatibility, excellent water dispersibility, and strong photostability, making them promising candidates for various applications, especially in biomedicine [1, 3].

To enhance emission efficiency and extend the emission range for potential applications, researchers have explored doping different

* Corresponding author.
E-mail address: lexuanhung@duytan.edu.vn

https://doi.org/10.25073/2588-1140/vnunst.5895

elements into GQDs. Doping with different atoms such as nitrogen, phosphorus, sulfur, iodine, boron, chlorine, and fluorine enables tuning various characteristics of GQDs, including their electronic, structural, and optical properties [1, 3, 4]. Previous studies have demonstrated that N-doping enhances fluorescence and improves biocompatibility. S-doping, however, is challenging, and fewer studies have been reported. Co-doping with both S and N has been attempted, but fabrication processes remain complex, and aqueous-phase precursors are rarely used. Additionally, the doping mechanism and its effect on GQDs' structure and properties remain insufficiently understood. Zihao Wang and his colleagues fabricated N-GQDs from dopamine hydrochloride using the hydrothermal method, resulting in yellow light emission for application as a fluorescent probe for detecting Fe^{3+}, which was used in biological imaging [5]. B-doped GQDs have been shown to increase photoluminescence intensity and achieve quantum efficiency up to 95% as reported by Yang and co-workers [6], because boron atoms are near carbon in the periodic table, allowing easy integration into the GQDs network. Additionally, P-GQDs have also been studied, with products fabricated by J. Liu's group showing good stability, dispersion and showed broad absorption in the visible light region [7].

Among the doping elements, nitrogen, being more electronegative, improves fluorescence quantum yield and enhances electron-donating characteristics [8]. Sulfur, with a larger atomic radius and different electronegativity, introduces mid-gap states and modulates emission behavior [9]. In addition, doping S into the GQDs network seems to be challenging, resulting in limited studies on S-GQDs. Shiyue Bian et al., fabricated S-GQDs with bright blue emission using the hydrothermal method with 1,3,6-trinitropyrene as a precursor of carbon, and MPA as a precursor of sulfur [10]. Recently, co-doping of heteroatom elements has been developed by many research groups. Co-doping helps extend emission range, introduce new surface states, and fine-tune the bandgap more effectively than single-element doping, thereby enhancing fluorescence intensity, photostability, and broadening potential applications. For co-doping nitrogen and sulfur into GQDs lies in their synergistic effect on tuning the electronic and optical properties [11]. Due to their strong and stable fluorescence in the visible region, excellent water dispersibility, and environmentally friendly synthesis method, the obtained N-GQDs and S,N-GQDs have promising potential in various applications such as bioimaging, fluorescence sensors, optoelectronic devices, and photocatalysis [11, 12]. A typical example is the co-doping of S and N, with many groups announcing the successful fabrication of GQDs co-doped with S and N [11, 13-15]. However, the fabrication process is complicated because the precursors are not liquid and easily use. Furthermore, the doping mechanism as well as the effect of co-doping on the structure and properties of the GQDs remain unclear.

In this study, we fabricated S,N-GQDs and N-GQDs using a new method that combines microwave-assisted pyrolysis with hydrothermal treatment. Microwave heating is a simple, fast and environmentally friendly method suitable for synthesizing quantum dots for biological applications. Combined with hydrothermal treatment, we have fabricated highly stable doped-GQDs. The doping mechanism, structure and optical properties of co-doped GQDs were discussed in detail.

2. Experimental

N-GQDs and S,N-GQDs were synthesized using a microwave-assisted hydrothermal method, employing citric acid (CA) as the carbon (C) source, urea as the nitrogen (N) source and thiourea as both the S and N source. The chemicals used were commercial products of high purity such as citric acid (99%), urea (99%), thiourea (99.5%) and double-distilled water. The preparation process followed a

method similar to that in publication [16]. For N-GQDs, a mixture of 0.01 mol CA and 0.03 mol urea was well mixed and pyrolyzed in a microwave at 500W. After melting into a colorless liquid, the mixture turns dark yellow and becomes a reddish-brown liquid after 1.5 minutes. This liquid was then quickly droped into double-distilled water under strong magnetic stirring for 15 minutes. The solution mixture was then placed into a Teflon flask, put in an autoclave and heated hydrothermally at 200 °C for 4 hours. After cooling to room temperature, a solution containing dark yellow N-GQDs was obtained. The same process was followed for the synthesis of S,N-GQDs using thiourea instead of urea. To clean the N-GQDs and S,N-GQDs, the synthesized solution was mixed with iso-propanol at a 1:4 volume ratio, shaken well and centrifuged at 11000 rpm. After washing, the samples were examined for characteristics to clarify the doping mechanism and evaluate the luminescence performance.

The morphology and size distribution of the S,N-GQDs and N-GQDs samples were analyzed using a JEOL JEM-2100 transmission electron microscope (TEM) operating at 200 kV. To prepare the samples for measurement, the solution was dropped onto a carbon-coated copper grid and dried at room temperature. Fourier transform infrared (FTIR) spectra were obtained using a Thermo Scientific's Nicolet iS10 FTIR spectrometer, spanning a wavenumber range of 4000 to 500 cm^{-1}. To analyze the atomic compostion and bonding in samples, X-ray photoelectron spectroscopy (XPS) was performed with a Thermo Fisher NX10, determining the atomic percentages of N, S, O and C. The ultraviolet-visible (UV-Vis) absorption spectra of samples dispersed in water were measured across the wavelength range of 200–1100 nm using an Agilent Cary 60 UV–Vis spectrophotometer. Photoluminescence (PL) spectroscopy was conducted with a on Horiba Jobin-Yvon Fluorolog-322 system, utilizing 450 W Xenon light with optional excitation wavelengths.

3. Results and Discussions

To investigate the optical characterization of doped-GQDs, N-GQDs and S,N-GQDs were fabricated using microwave combine hydrothermal in an aqueous medium. After fabrication, the samples were initially analyzed for their structure and morphology. TEM images of S,N-GQDs and N-GQDs are shown in Figure 1a and 1b, respectively. Analysis revealed that N-GQDs average approximately 4.5 nm in size, whereas S,N-GQDs exhibit an average size of approximately 9.5 nm. Figure 1c presents the FTIR spectra of two samples, S,N-GQDs and N-GQDs. The vibrations of the main bonds confirm the formation of GQD network, with *C=C* stretching of graphite at 1548 cm^{-1} for S,N-GQDs and approximately 1553 cm^{-1} for N-GQDs. The *C=O* and *C–O* stretching vibrations were also observed at 1653 cm^{-1}, 1192 cm^{-1} for S,N-GQDs and 1660 cm^{-1}, 1190 cm^{-1} for N-GQDs, respectively [17-19]. The doping of N into the graphene lattice is confirmed by the vibrations of the *C=N* bonds at 1394 cm^{-1}. The co-doping of S and N into the graphene lattice is confirmed by the *C=N* and *C=S* bonds at 1186 and 1020 cm^{-1}, respectively [11, 19]. The broad peak ranging from 2900 to 3200 cm^{-1} is attributed to the stretching vibration of hydrogen-bonded OH groups from adsorbed water (including *O–H* and *N–H* stretching vibrations) [19, 20]. The aromatic nucleus is observed in the low-frequency regions around 597 and 644 cm^{-1}. When co-doping S and N atoms, an additional peak at 1020 cm^{-1} appears in the FTIR spectrum, which is not present in the N-GQDs samples. These results suggest that N and S atoms were successfully incorporated into the graphene lattice, forming the corresponding bonds. The FTIR findings confirm that S and N can be effectively doped into GQDs.

To further characterize the surface chemistry, XPS was used to analyze composition of S,N-GQDs and N-GQDs. The surface elemental composition in atomic percentages, along with the deconvolution

results of C 1s, O 1s, S 2p and N 1s core energy level spectra, are detailed in Table 1 and Figure 2. Figure 2 shows the XPS curves of the two samples, S,N-GQDs and N-GQDs, prepared in an aqueous medium. The full scan XPS spectra of the S,N-GQDs and N-GQDs (Figure 2a) exhibit four peaks at 284.7 eV, 532 eV, 399 eV and 163.46 eV, corresponding to C1s, O 1s, N 1s and S 2p, respectively. These peaks can be observed in the XPS survey spectra of N-GQDs and of S,N-GQDs, similar to those observed as reported in [21, 22]. For the S,N-GQDs sample, the XPS spectrum confirms the presence of C, O, N and S with the atomic concentration of 55.5%, 30%, 11.7%, 2.8% respectively. For the N-GQDs sample, the atomic concentrations of C, O and N are 60.2%, 29.9% and 9.9%, respectively (Table 1).

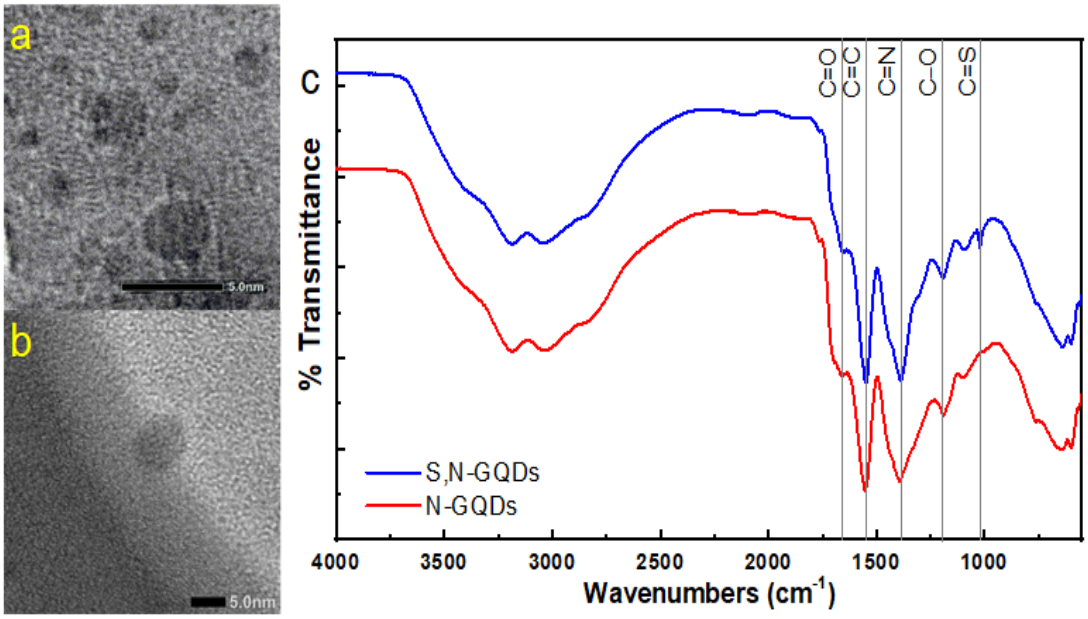

Figure 1. TEM image of N-GQDs (a), S,N-GQDs(b), and the FTIR spectra (c) of these synthesized samples.

The deconvolution analysis of C 1s**,** O 1s, N 1s and S 2p spectra for S,N-GQDs and N-GQDs were also performed, as shown in Figure 2b, c, d. For S,N-GQDs, the deconvoluted C 1s spectra comprised a non-oxygenated ring (*C-C/C=C*, 284.8 eV), *C-N* bonds (288.2 eV), and carboxylate (*O=C-O*, 291.2 eV). The deconvoluted O1s spectra showed *C=O* bond (531.3 eV), *C-OH/C-O-C* bond (532.1 eV). The deconvoluted N 1s spectra comprised NH_2/pyrrolic N (399.5 eV) and graphitic N (400.2 eV), as reported in [22]. The deconvolution of the S 2p orbit (insert Figure 2a) revealed two peaks located at 163.6 and 167.8 eV, corresponding to *C-S-C* $2p_{1/2}$ bonding and *S=O*, respectively [22-24]. All deconvolution of the C 1s, O 1s, N 1s and S 2p peaks and the corresponding binding energies are presented in Table 1**.** For the N-GQDs, the deconvoluted C 1s spectra comprised a non-oxygenated ring (*C-C/C=C*, 284.5 eV), *C-N* bonds (287.8 eV), and carboxylate (*O=C-O*, 291.5 eV). The deconvoluted O 1s shows *C=O* bond (531.3 eV) and *C-OH/C-O-C* bond (532.1 eV). The deconvoluted N 1s spectra comprised NH_2/pyrrolic N (399.5 eV) and graphitic N (400.2 eV) as reported in [22]. These findings verify the effective doping of sulfur and nitrogen into the GQDs framework, corroborating the FTIR analysis results. Thus, we can conclude that the samples fabricated and used in this study are N-GQDs and S,N-GQDs.

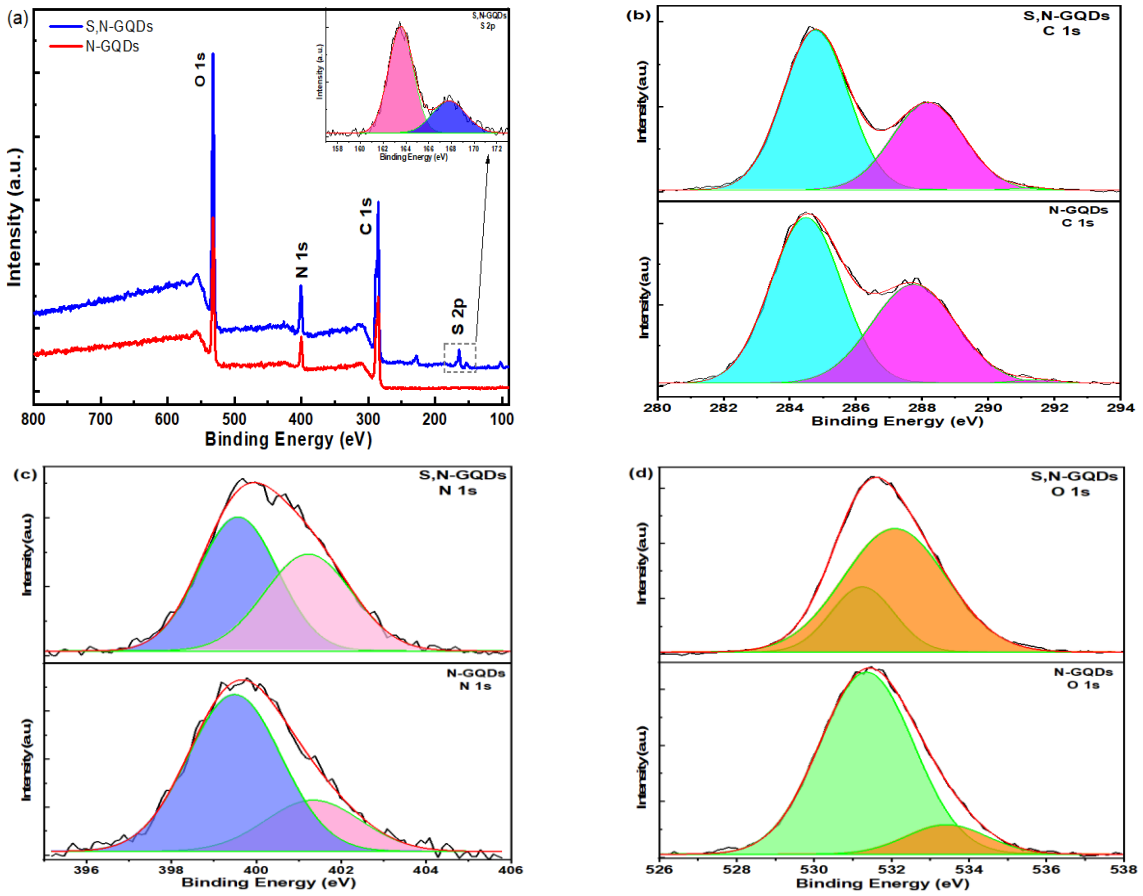

Figure 2. XPS spectra of the two samples of N-GQDs and S,N-GQDs and the deconvoluted high-resolution spectra of C 1s, O 1s, N 1s and S 2p orbits and the fitted peaks using Gaussian function.

Effects of heteroatoms on the optical characterization of N-GQDs, and S,N-GQDs were investigated by absorption, photoluminescence (PL) and photoluminescence excitation (PLE) spectra, as displayed in Figure 3 and Figure 4. First, the absorbance spectra are presented in Figure 3 that shows important differences appear between N doped and S, N co-doped GQDs. The spectrum of N-GQDs samples shows peaks located at approximately λ=235 nm (π-π* transition of aromatic *C=C* bonds), and at 332 nm (n-π* transition of aromatic *C=O* bonds). The absorption spectrum of S,N co-doped GQDs samples shows an additional peak at 338 nm, which is attributed to the n– π* transition from $C\pi \rightarrow O\pi$*. Thus, when GQDs doped with N or co-doped with S, N, there are additional transitions such as $C\pi \rightarrow N\pi$* or $C\pi \rightarrow S\pi$* transitions, alongside the primary $C\pi \rightarrow C\pi$* transition. This results in red shift of the emission peak. Additionally, absorption peaks due to Cπ → Oπ* electronic transitions occur from the present *C=O* and *C–O* groups [25-30] or the surface states [31].

The PL band of the N-GQDs is located at 440 nm. By co-doping S and N (S,N-GQDs), the emission band shifts to a higher wavelength of 458 nm (Figure 4). This shift indicates that S and N co-doping creates lower energy levels compared to N doping alone, causing a red shift

in the emission peak [25-27]. This PL band can be attributed to the combined emission transition from energy levels in both S-GQDs and N-GQDs samples. In the PLE spectra (insert Figure 4), both N doped and S, N co-doped samples exhibit two bands that absorb and emit more light at wavelengths around 280-320 nm and 350-400 nm.

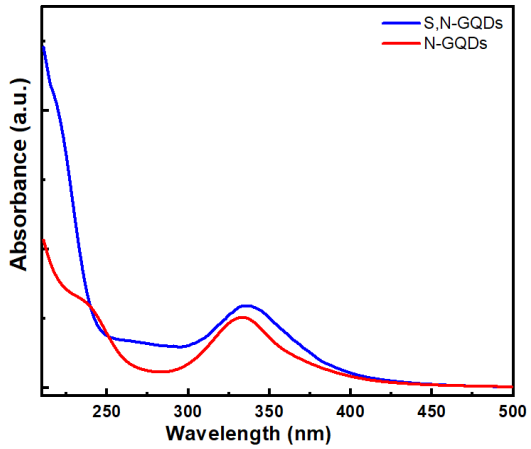

Figure 3. UV-vis absorption spectra of the S,N-GQDs and N-GQDs samples prepared in aqueous medium.

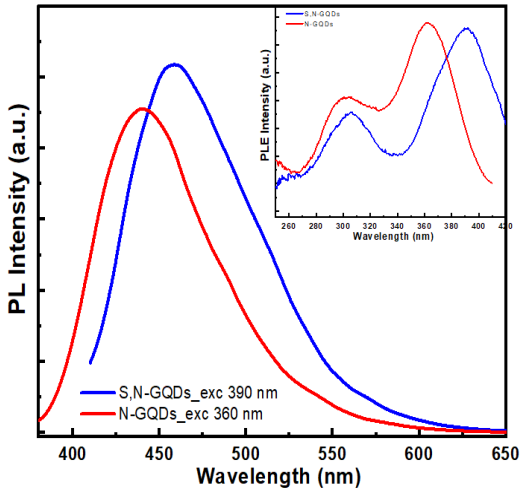

Figure 4. PL emission spectra of the S,N-GQDs and N- GQDs samples prepared in aqueous medium.

This suggests that doping with N or co-doping with S and N, introduces additional $C\pi \rightarrow N\pi^*$ and $C\pi \rightarrow S\pi^*$ transition along with the primary $C\pi \rightarrow C\pi^*$ emission transition, resulting in a shift towards longer wavelength in the emission peak. The emitted band is a superposition of the two transitions: $\pi^* \rightarrow \pi$ and $n \rightarrow \pi$ [32]. Furthermore, the deconvolution of the O 1s spectra reveals that co-doping with S and N decreases the *C-O* functional group while increasing the *C=O* function. This change causes the redshift observed in the S,N co-doped sample [13, 25]. This mechanism is illustrated in the proposed energy level diagram (Figure 5), where the dopant-induced n states—corresponding to Oπ*, Nπ*, and Sπ* orbitals—are located between the intrinsic π and π* levels of the carbon framework. These intermediate states enable additional radiative transitions at lower energies, which account for the observed redshift and excitation-dependent photoluminescence behavior. Such results are consistent with recent studies that have similarly attributed the emission mechanisms of doped GQDs to the presence of these mid-gap states [12, 32].

Table 1. The deconvolution of C 1s, N 1s, O 1s and S 2p peaks of XPS spectraof co-doped samples and their C, N, O and S bonding composition

Deconvolution of peak	Attribute	S,N-GQDs	N-GQDs
C 1s	(C-C/C=C)	284.78	284.49
	(C-N)	288.18	287.75
	(C=O)	291.22	291.46
	C at. %	**55.5**	**60.2**
O 1s	C=O/O–H	531.25	531.36
	C–O	532.09	533.43
	O at. %	**30**	**29.9**
N 1s	(C-N-C)	399.57	399.35
	(N-C_3)	401.23	400.23
	N at. %	**11.7**	**9.9**
S 2p	$2p_{3/2}$	163.56	
	$2p_{1/2}$	167.81	
	S at. %	**2.8**	

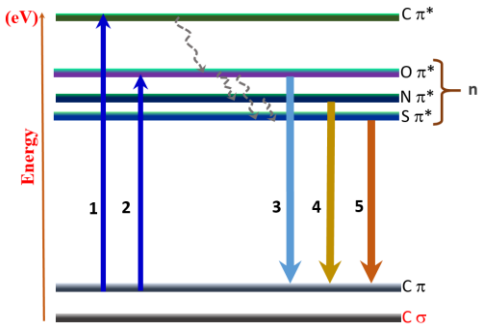

Figure 5. Schematic energy level diagram illustrating the redshifted photoluminescence behavior of N-GQDs and S,N-GQDs. Arrows ①–② represent absorption transitions to π and dopant-induced n-type states; arrows ③–⑤ indicate radiative emissions from Oπ, Nπ*, and Sπ* states to the π ground state.

Figure 6 illustrates the excitation and emission contour maps of PL intensity for the S,N-GQD (left) and N-GQDs (right) prepared in aqueous medium. These maps revral the samples' maximum efficiency bands. For S,N-GQD sample, the emission peak is around 450-500 nm for all excitation wavelengths, with the most intense PL emission occurring at excitation wavelengths around 420 nm. The map shows that the emission's position and intensity are highly dependent on the excitation wavelength. Conversely, N-GQDs exhibit a emission peak around 450 nm, emiting most intensely at 360 nm, with the emission position remaining relatively constant despite changes in the excitation wavelength.

While the emission intensity depends strongly on the excitation wavelength, the emission position is almost independent of it. It can be seen that doping GQDs with N or co-doping with S and N leads to a redshift in the absorption and fluorescence spectra. This redshift is due to the formation of *n* levels corresponding to the *Oπ**, *Nπ**, *Sπ** states, which are located between *π* and *π** levels of carbon [32]. The prepared samples are well suited for optical applications in the visible region, exhibiting significant and stable emission at 450-500 nm (stable) when excited at 360-420 nm.

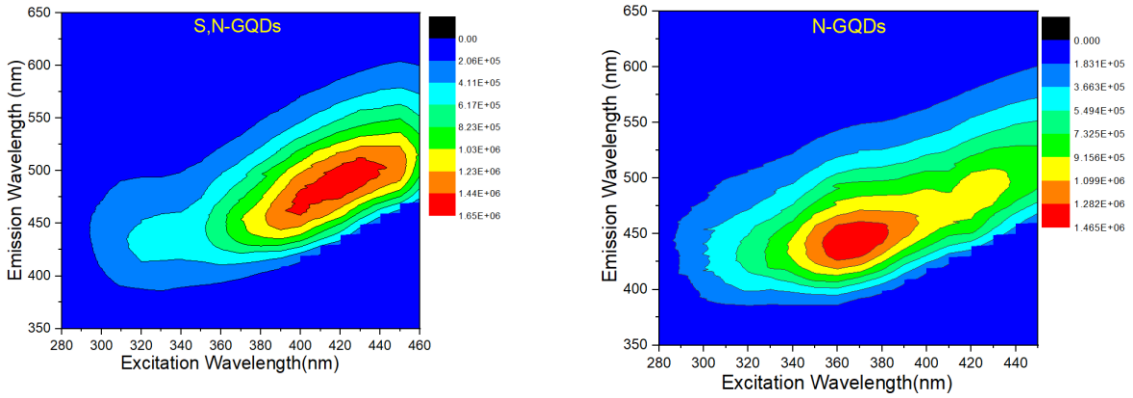

Figure 6. EEM images of S,N-GQDs (left) and N-GQDs (right) samples fabricated in aqueous medium.

4. Conclusion

In summary, by using microwave-assisted pyrolysis combined with hydrothermal treatment in water, N-GQDs and S,N-GQDs samples were successfully fabricated with simple, easy-to-find initial precursors. The fabricated samples exhibit a strong absorption peak at 332-338 nm, depending on the type of dopants, and demonstrate strong luminescence intensity at 440 and 458 nm, respectively. The fluorescence, absorption spectrum and EEM analysis indicate that the absorption peak is caused by the transitions *Cπ* → *Cπ** and *Cπ* →

$O\pi^*$, while the fluorescence peak is due to the formation of impurities between $C\pi$ and $C\pi^*$.

Acknowledgements

This research is funded by Vietnam National Foundation for Science and Technology Development (NAFOSTED) under grant number 103.03-2020.22.

References

[1] P. Tian, L. Tang, K. S. Teng, S. P. Lau, Graphene Quantum dots from Chemistry to Applications, Materials Today Chemistry, Vol. 10, 2018, pp. 221-258.

[2] Z. Geng, B. H¨ahnlein, R. Granzner, M. Auge, A. A. Lebedev, V. Y. Davydov, M. Kittler, J.o. Pezoldt, F. Schwierz, Graphene Nanoribbons for Electronic Devices, Ann. Phys. (Berlin) Vol. 529, 2017, pp. 1700033.

[3] S. Zhu, Y. Song, X. Zhao, J. Shao, J. Zhang, B. Yang, The Photoluminescence Mechanism in Carbon Dots (Graphene Quantum Dots, Carbon Nanodots, and Polymer Dots): Current State and Future Perspective, Nano Research, Vol. 8, No. 2, 2015, pp. 355–381.

[4] H. Y. Nguyen, X. H. Le, N. T. Dao, N. T. Pham, T. H. H. Vu, N. H. Nguyen, T. N. Pham, Microwave-Assisted Synthesis of Graphene Quantum Dots and Nitrogen-Doped Graphene Quantum Dots: Raman Characterization and Their Optical Properties, Advances in Natural Sciences: Nanoscience and Nanotechnology, Vol. 10, No. 2, 2019, pp. 025005.

[5] Z. Wang, D. Chen, B. Gu, B. Gao, Z. Liu, Y. Yang, Q. Guo, X. Zheng, G. Wang, Yellow Emissive Nitrogen-Doped Graphene Quantum Dots as a Label-Free Fluorescent Probe for Fe^{3+} Sensing and Bioimaging, Diamond and Related Materials, Vol. 104, 2020.

[6] Z. Fan, Y. Li, X. Li, L. Fan, S. Zhou, D. Fang, S. Yang, Surrounding Media Sensitive Photoluminescence of Boron-Doped Graphene Quantum Dots for Highly Fluorescent Dyed Crystals, Chemical Sensing and Bioimaging, Carbon, Vol. 70, 2014, pp. 149-156.

[7] J. Qian, C. Shen, J. Yan, F. Xi, X. Dong, J. Liu, Tailoring the Electronic Properties of Graphene Quantum Dots by P Doping and Their Enhanced Performance in Metal-Free Composite Photocatalyst, The Journal of Physical Chemistry C, Vol. 122, No. 1, 2017, pp. 349-358.

[8] X. Liu, B. Sun, One-Pot Synthesis of Nitrogen-Doped Graphene Quantum Dots and Their Applications in Bioimaging and Detecting Copper Ions in Living Cells, ACS Omega, Vol. 8, No. 30, 2023, pp. 27333-27343.

[9] S. Bian, C. Shen, H. Hua, L. Zhou, H. Zhu, F. Xi, J. Liu, X. Dong, One-Pot Synthesis of Sulfur-Doped Graphene Quantum Dots as a Novel Fluorescent Probe for Highly Selective and Sensitive Detection of Lead(Ii), RSC Advances, Vol. 6, No. 74, 2016, pp. 69977-69983.

[10] S. Bian, C. Shen, Y. Qian, J. Liu, F. Xi, X. Dong, Facile Synthesis of Sulfur-Doped Graphene Quantum Dots as Fluorescent Sensing Probes for Ag^+ Ions Detection, Sensors and Actuators B: Chemical, Vol. 242, 2017, pp. 231-237.

[11] T. Selvakumar, M. Rajaram, A. Natarajan, L. Harikrishnan, K. Alwar, A. Rajaram, Highly Efficient Sulfur and Nitrogen Codoped Graphene Quantum Dots as a Metal-Free Green Photocatalyst for Photocatalysis and Fluorescent Ink Applications, ACS Omega, Vol. 7, No. 15, 2022, pp. 12825-12834.

[12] M. M. Farahani, F. Ghorbani, N. Mosleh, Boric Acid Modified S and N Co-Doped Graphene Quantum Dots as Simple and Inexpensive Turn-On Fluorescent Nanosensor for Quantification of Glucose, Spectrochim Acta a Mol Biomol Spectrosc, Vol. 245, 2021, pp. 118892.

[13] H. S. Hojaghan, O. Amiri, M. Hassanpour, M. P. Kalamuei, H. Moayedi, M. S. Niasari, S,N Co-Doped Graphene Quantum Dots-Induced Ascorbic Acid Fluorescent Sensor: Design, Characterization and Performance, Food Chem, Vol. 295, 2019, pp. 530-536.

[14] S. Sajjadi, A. Khataee, R. Darvishi Cheshmeh Soltani, A. Hasanzadeh, N, S Co-Doped Graphene Quantum Dot–Decorated Fe_3O_4 Nanostructures: Preparation, Characterization and Catalytic Activity, Journal of Physics and Chemistry of Solids, Vol. 127, 2019, pp. 140-150.

[15] Z. Ouyang, Y. Lei, L. Luo, Z. Jiang, J. Hu, Y. Lin, S, N Co-Doped Graphene Quantum Dots Decorated Cdse for Enhanced Photoelectric Properties, Nanotechnology, Vol. 31, No. 9, 2020, pp. 095710.

[16] L. X. Hung, N. H. Yen, T. T. Hue, D. N. Thuan, P. N. Thang, V. T. H. Hanh, V. C. Nhung, J. Laverdant, N. T. M. Huong, P. T. Nga, Fabrication and Optical Properties of Sulfur- and Nitrogen-Doped Graphene Quantum Dots by The Microwave–Hydrothermal Approach, Journal of Nanoparticle Research, Vol. 24, No. 10, 2022, pp. 206.

[17] M. T. Hasan, R. G. Rodriguez, C. Ryan, K. Pota, K. Green, J. L. Coffer, A. V. Naumov, Nitrogen-Doped Graphene Quantum Dots: Optical Properties Modification and Photovoltaic Applications, Nano Research, Vol. 12, No. 5, 2019, pp. 1041-1047.

[18] Z. Yang, M. Xu, Y. Liu, F. He, F. Gao, Y. Su, H. Wei, Y. Zhang, Nitrogen-Doped, Carbon-Rich, Highly Photoluminescent Carbon Dots from Ammonium Citrate, Nanoscale, Vol. 6, No. 3, 2014, pp. 1890-1895.

[19] S. S. Dwitya, Y. H. Hsueh, S. S. S. Wang, K. S. Lin, Ultrafine Nitrogen-Doped Graphene Quantum dot Structure and Antibacterial Activities Against Bacillus Subtilis 3610, Materials Chemistry and Physics, Vol. 295, 2023, pp. 127135.

[20] M. He, J. Zhang, H. Wang, Y. Kong, Y. Xiao, W. Xu, Material and Optical Properties of Fluorescent Carbon Quantum Dots Fabricated from Lemon Juice via Hydrothermal Reaction, Nanoscale Res Lett, Vol. 13, No. 1, 2018, pp. 175.

[21] W. Zhu, X. Feng, M. Zhao, Z. Wei, Z. Liu, G. Wang, Q. Guo, D. Chen, Scalable and Atom Economic Preparation of Red-Near-Infrared Emitted N-Doped Graphene Quantum Dots with a High Quantum Yield, Diamond and Related Materials, Vol. 116, 2021, pp. 108395.

[22] Z. Ouyang, Y. Lei, Y. Chen, Z. Zhang, Z. Jiang, J. Hu, Y. Lin, Preparation and Specific Capacitance Properties of Sulfur, Nitrogen Co-Doped Graphene Quantum Dots, Nanoscale Res Lett, Vol. 14, No. 1, 2019, pp. 219.

[23] Y. Su, Y. Zhang, X. Zhuang, S. Li, D. Wu, F. Zhang, X. Feng, Low-Temperature Synthesis of Nitrogen/Sulfur Co-Doped Three-Dimensional Graphene Frameworks as Efficient Metal-Free Electrocatalyst for Oxygen Reduction Reaction, Carbon, Vol. 62, 2013, pp. 296-301.

[24] Z. Yang, Z. Yao, G. Li, G. Fang, H. Nie, Z. Liu, X. Zhou, X.a. Chen, S. Huang, Sulfur-Doped Graphene as an Efficient Metal-free Cathode Catalyst for Oxygen Reduction, ACS Nano, Vol. 6, No. 1, 2012, pp. 205-211.

[25] P. R. Kharangarh, S. Umapathy, G. Singh, Thermal Effect of Sulfur Doping for Luminescent Graphene Quantum Dots, ECS Journal of Solid State Science and Technology, Vol. 7, No. 3, 2018, pp. M29-M34.

[26] P. R. Kharangarh, S. Umapathy, G. Singh, Investigation of Sulfur-Related Defects in Graphene Quantum Dots for Tuning Photoluminescence and High Quantum Yield, Applied Surface Science, Vol. 449, 2018, pp. 363-370.

[27] R. Das, S. Parveen, A. Bora, P. K. Giri, Origin of High Photoluminescence Yield and High SERS Sensitivity of Nitrogen-Doped Graphene Quantum Dots, Carbon, Vol. 160, 2020, pp. 273-286.

[28] S. Kadian, G. Manik, K. Ashish, M. Singh, R. P. Chauhan, Effect of Sulfur Doping on Fluorescence and Quantum Yield of Graphene Quantum Dots: An Experimental and Theoretical Investigation, Nanotechnology, Vol. 30, No. 43, 2019, pp. 435704.

[29] S. Kadian, G. Manik, A Highly Sensitive and Selective Detection of Picric Acid Using Fluorescent Sulfur-Doped Graphene Quantum Dots, Luminescence, Vol. 35, No. 5, 2020, pp. 763-772.

[30] X. Li, S.P. Lau, L. Tang, R. Ji, P. Yang, Sulphur Doping: A Facile Approach to Tune The Electronic Structure and Optical Properties of Graphene Quantum Dots, Nanoscale, Vol. 6, No. 10, 2014, pp. 5323-5328.

[31] S. Kang, Y. K. Jeong, K. H. Jung, Y. Son, W. R. Kim, J. H. Ryu, K. M. Kim, One-Step Synthesis of Sulfur-Incorporated Graphene Quantum Dots Using Pulsed Laser Ablation for Enhancing Optical Properties, Opt Express, Vol. 28, No. 15, 2020, pp. 21659-21667.

[32] T. Vu Tuyet Nhung, H. Van Tuyen, N. Tran, L. Xuan Hung, S, N Co-Doped Graphene Quantum Dots Fabricated by Rapid Microwave-Assisted Pyrolysis and Their Optical Properties, Materials Today Communications, Vol. 37, 2023, pp. 107282.